Characterization of ABS + W and ABS + Bi 3D printing filaments attenuation for different photon beams

Villani, D. 1; Savi, M.[1,2]; Andrade, M. A. B. [2] Campos, L.L.[1] and Potiens, M. P. A.[1]

[1] Instituto de Pesquisas Energéticas e Nucleares – IPEN. Avenida Lineu Prestes, 2242 Cidade Universitária. 05508-000. São Paulo – SP, Brazil.

[2] Instituto Federal de Santa Catarina – IFSC. Avenida Mauro Ramos, 950. Centro, 88020-300. Florianópolis – SC, Brazil

matheus.savi@ifsc.edu.br

Abstract. 3D printing techniques and materials have become widely available in the last couple of decades and remains a hot topic of study as new materials can lead to new applications. This study aims to evaluate the attenuation behaviour of GMASS over photon beams ranging from 29.7 up to 661.7keV, comparing with pure ABS and using theoretical data of pure lead as reference. It was used the transmission method to obtain experimental attenuation coefficients to all materials and theoretical data. HVL and TVL calculations were also performed. Results show that ABS+W has higher attenuation than ABS+Bi and pure ABS. Using the lead theoretical reference data it can be concluded that although ABS+Bi and ABS+W attenuates less than pure lead, the 3D printing filaments can be used to create shielding tolls depending on radiation energy and application.

Keywords. 3D printing, GMASS, ABS, attenuation coefficients.

1. Introduction

Although 3D printing was created in 80's [1,2], just in the 21 century it became widely available [3] since some patents felt and many companies start to develop their own machines and correlated products. This started a revolution in many knowledge areas, especially in industry and medical fields.

There are many kinds of 3D printing technologies, but Fused Filament Fabrication (FFF) appear as the most common worldwide, as the costs of machinery and inputs are less expensive than others available.

With the spread of this technique, many innovations for use in FFF became accessible to general public, like better printers (extrusion types, printer beds and multimaterial support) and a wide variety of new filaments for specific uses, as GMASS [4] for radiation shielding and XCT [5] for bone equivalency for diagnostic and dosimetry purposes. GMASS filaments are commercially available mainly in United States, where they are fabricated. They are composed of Acrylonitrile-Butadiene-Styrene (ABS) as base polymer and added in weight 70 to 78% of Bismuth Oxide - Bi_2O_3 (Bi) or Tungsten powder (W).

Thus, this study aims to evaluate the behavior of attenuation of GMASS 3D printing filaments over four reference qualities of X-ray in the diagnostic energy range, one gamma energy and theoretical data for pure lead as reference. The linear attenuation coefficients of the materials is determined and compared with ABS filament without additives.

2. Experimental

2.1. 3D printing materials and printing set-up

Eight plates of each material (ABS, ABS+Bi and ABS+W) (Figure 1) were printed with dimensions of 40 x 40 x 1 mm³ and 100% rectilinear (+45º/-45º) infill in a Flashforge Creator Pro 3D and compared for radiation attenuation characteristics. The details of the 3D printing filaments and protocols can be found in Table 1.

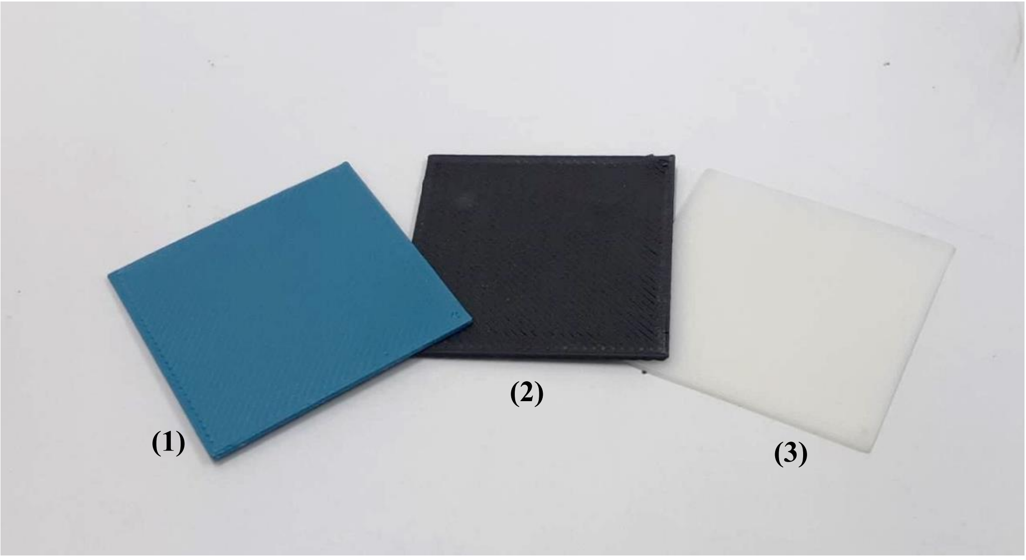

Figure 1. 3D printed plates used in this study. (1) ABS+Bi (2) ABS+W and (3) pure ABS

Table 1. Printing set-up characteristics used

Material	Producer	Nominal Density (g/cm^3)	Nozzle Temperature (ºC)	Heated Bed Temperature (ºC)	Print Speed (mm/s)
ABS	3DON	1.04	210 - 250	80 - 110	50
ABS+Bi	Turner Medtech	2.70	210 - 230	100-110	40
ABS+W		4.00	210 - 230	100-110	70

2.2. Radiation beams

For this study, it was used RQR standard x-ray qualities [6] and ^{137}Cs gamma rays to allow the knowledge of attenuation behavior of the 3D printing filaments from a wide photon energy spectrum. The RQR standard radiation qualities and 661.7keV gamma rays were obtained using the X-ray system Pantak/Seifert ISOVOLT 160 HS and ^{137}Cs irradiator from the Instruments Calibration Laboratory – LCI/IPEN. Details on the radiation beams are showed in Table 2. Theoretical values of attenuation were also obtained for pure lead as comparison using Spektr 3.0 computational toolkit [7] for the RQR standard beams.

Table 2. Reference radiation qualities used in this study

Radiation Quality (X-rays)	Tube voltage (kVp)	HVL (mmAl)	Additional Filtration (mm)	Mean photon energy (keV)
RQR 3	50	1.78	2.4Al	29.7
RQR 5	70	2.58	2.8Al	34.0
RQR 8	100	3.97	3.2Al	38.1
RQR 10	150	6.57	4.2Al	46.5
Beam Quality (γ-rays)	**Nominal Activity (GBq)**		**Mean photon energy (keV)**	
^{137}Cs	740.0 at 28th april 1995		661.7	

2.3. Radiation detection systems

To obtain the experimental data related to the radiation transmitted from the attenuated beams it was used two commercial radiation detection systems. For the RQR standard beams it was used a RaySafe X-ray detection system with X2 R/F solid state sensor connected. The ^{137}Cs gamma rays were detected using a RADCAL ion chamber 6cc 10X5-6 connected to a RADCAL 9015 electrometer.

2.4. Irradiation set-up and data analysis

The transmission method was used to determine the linear attenuation coefficients of the printing filaments for the photon radiation qualities studied.

The 3D printed plates thickness was increased from zero (without absorber) to 10 mm and positioned in front of the beam exit. The values obtained in this procedure were analysed using Origin® 9.1 software. For each quality an exponential fit was performed in order to obtain the linear attenuation coefficients according to Eq. 1

$$I = I_0 e^{-\mu x} \quad \text{(Eq. 1)}$$

where I_0 is the initial beam intensity, and I is the beam intensity when some material of thickness x was placed between radiation source and radiation detector. Once the linear attenuation coefficients are calculated, the experimental values of half-value layer (HVL) and tenth-value layer (TVL) for the filaments can be obtained using Eq. 2 and 3 respectively

$$HVL = \frac{ln\,(2)}{\mu} \quad \text{(Eq. 2)}$$

$$TVL = \frac{ln\,(10)}{\mu} \quad \text{(Eq. 3)}$$

Figure 2 show the irradiation set-ups for both Pantak X-ray system and the ^{137}Cs irradiator.

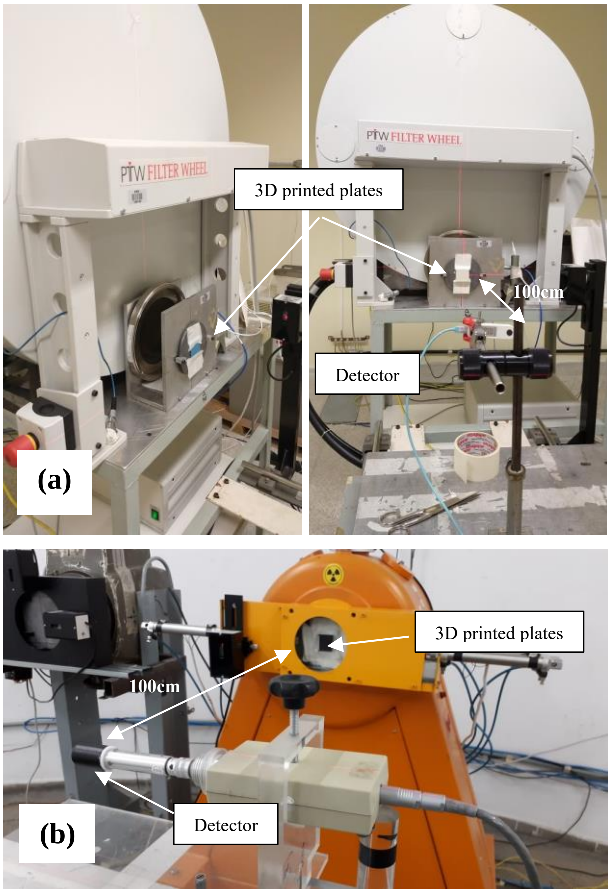

Figure 2. Irradiation set-up for the transmission measurements. (a) Pantak (b) ^{137}Cs gamma irradiator. Source/beam exit – beam detection distances used were 100cm. The attenuation 3D printed plates were positioned at the beam exits

3. Results

3.1. Radiation transmissions

Figures 3 to 5 show the experimental results on radiation transmission for ABS, ABS + Bi and ABS + W respectively. Figure 6 show the theoretical transmission with lead obtained with Spektr computational toolkit. Applying an exponential fit to the points using Eq. 1, the attenuation coefficient data for the different beam qualities were obtained and the results are shown in Table 3. The presented exponential fits resulted in $R^2 \geq 0.999$, showing great agreement between calculated and experimental data.

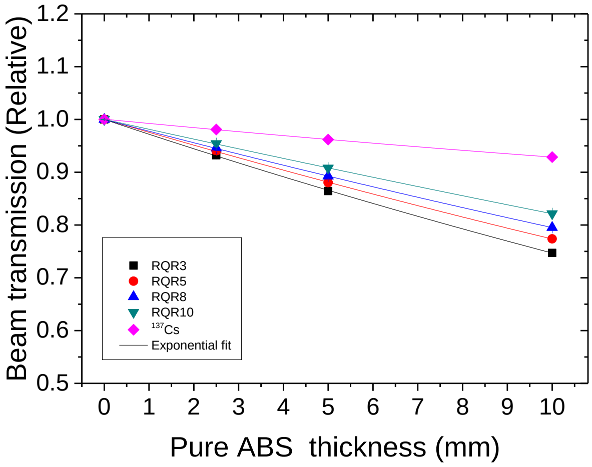

Figure 3. Radiation transmissions obtained with ABS

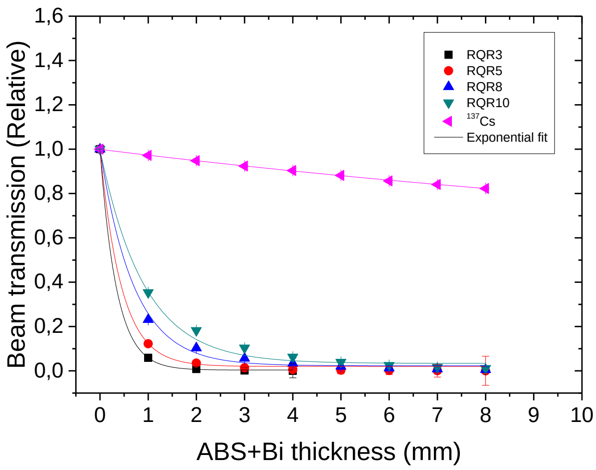

Figure 4. Radiation transmissions obtained with ABS + Bi

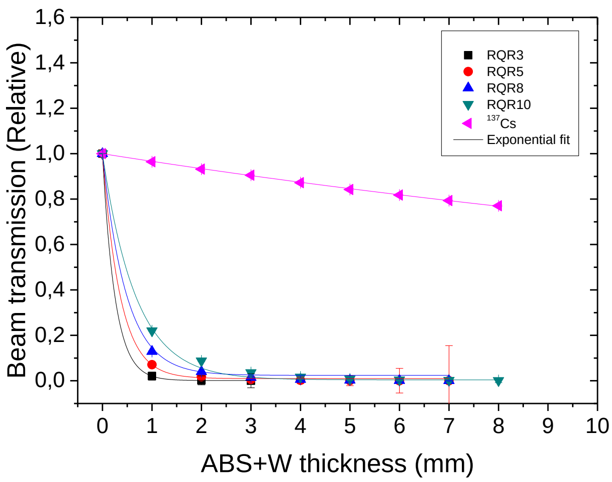

Figure 5. Radiation transmissions obtained with ABS + W

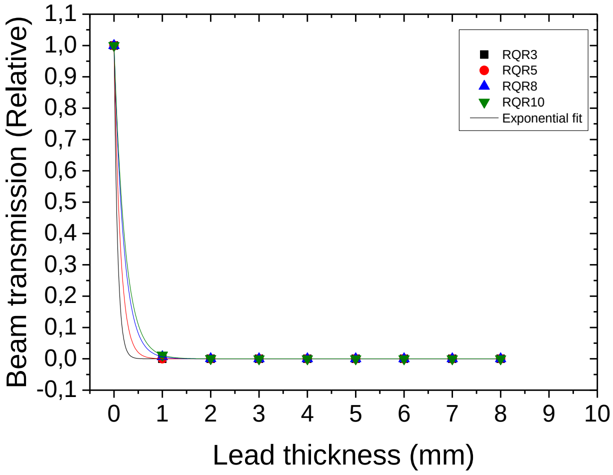

Figure 6. Theoretical radiation transmissions obtained with pure lead using Spektr 3.0

Table 3. Experimental linear attenuation coefficients (μ)

Radiation Quality	ABS		ABS + Bi		ABS + W		Lead [7]	
	μ (mm^{-1})	**σ**	**μ (mm^{-1})**	**σ**	**μ (mm^{-1})**	**σ**	**μ (mm^{-1})**	**σ**
RQR3	0.024	0.006	2.893	0.027	3.935	0.012	13.7604	0.00002
RQR5	0.021	0.005	2.246	0.052	2.786	0.041	7.749	0.003
RQR8	0.019	0.002	1.420	0.080	2.078	0.063	5.005	0.020
RQR10	0.011	0.003	1.095	0.033	1.477	0.006	4.415	0.018
^{137}Cs	0.004	0.007	0.051	0.006	0.044	0.010	-	-

3.2. Energy dependence on the materials

Comparing the coefficients obtained, it is possible to observe the differences on behavior of the transmission of the materials to the different qualities of radiation and, consequentially, though the energy range from ~30 keV to 661.7 keV. Using the experimental information obtained, Figure 6 show the energy dependence on behavior of the attenuation of the materials. Results are relative to ^{137}Cs.

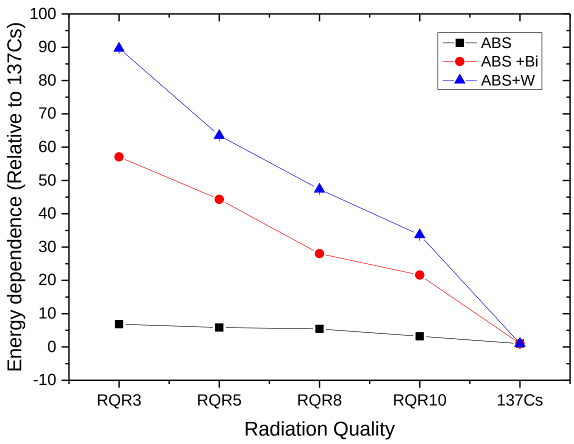

Figure 6. Energy dependence of the printing materials

3.3. HVL and TVL calculations

Using the attenuation coefficients (μ) of Table 3 and equations 2 and 3, the experimental values of HVL and TVL to the printing materials were calculated and the results can be found in Tables 4 and 5.

Table 4. Experimental half value layer (HVL) obtained

Radiation Quality	ABS		ABS + Bi		ABS + W		Lead	
	HVL (mm)	σ	HVL (mm)	σ	HVL (mm)	σ	HVL (mm)	σ
RQR3	28.65429	0.00015	0.240	0.079	0.176	0.047	0.0504	0.0002
RQR5	33.59899	0.00009	0.309	0.117	0.249	0.115	0.089	0.024
RQR8	36.27144	0.00003	0.488	0.114	0.334	0.132	0.139	0.010
RQR10	61.17804	0.00004	0.633	0.036	0.469	0.009	0.157	0.079
^{137}Cs	196.3590	0.00003	13.6742	0.0003	15.7964	0.0004		

Table 5. Experimental tenth value layer (TVL) obtained

Radiation Quality	ABS		ABS + Bi		ABS + W		Lead	
	TVL (mm)	σ	TVL (mm)	σ	TVL (mm)	σ	TVL (mm)	σ
RQR3	95.18748	0.00004	0.796	0.024	0.585	0.014	0.167	0.050
RQR5	111.61343	0.00003	1.025	0.035	0.827	0.035	0.297	0.096
RQR8	120.49111	0.00001	1.621	0.034	1.108	0.040	0.460	0.096
RQR10	203.22905	0.00001	2.103	0.011	1.559	0.003	0.522	0.008
^{137}Cs	652.2904	0.00001	45.4248	0.0001	52.4746	0.0001		

4. Discussion

The 3D printing filaments used in this study are ABS based. When Bismuth or Tungsten are added to the polymer matrix of the filaments, the known properties of these two materials for radiation protection at certain energies are aggregated on the ABS basis and can be used with 3D printing. Even though ABS had a slightly low radiation attenuation for the studied photon energies, the ABS + Bi and ABS + W filaments showed good attenuation making a 50% reduction of the diagnostic X-ray with less than 1 mm.

Analyzing the energy dependency of the attenuation of the materials one can notice that ABS+W printed plates attenuates up to 90 times more than pure ABS and approximately 30 times more than ABS + Bi for RQR3 and these values decreases as the peak voltage increases. Despite of the less visible differences between the attenuation coefficients for ^{137}Cs gamma radiation, both ABS + W and ABS + Bi decreases the transmitted signal approximately 9 times more than pure ABS.

As less than 1mm of absorber are need to ABS + Bi and ABS + W obtain a HVL for diagnostic radiology beams and the curve at this region had a high decay, the only way to determine this values are by calculation, what led a high uncertainties when compared with ^{137}Cs. Values obtained for TVL enables for diagnostic radiology energy qualities and probably for gamma radiation up to ^{99m}TC the production of accessories for shielding and filtration, with near a maximum of 2.5 mm of ABS + Bi and approximately 1.5 mm of ABS + W.

5. Conclusions

In according to the results presented in this study ABS+W is a better absorber of radiation than ABS + Bi and pure ABS. With the HVL and TVL values it is possible to design by 3D printing a new row of parts and accessories for radiation shielding, especially for photons ranging on diagnostic radiology energies.

Acknowledgments

The authors would like to thank IFSC, IPEN, CAPES (558/2018), FAPESP (PROJECT 2017/50332-0) and CNPq (PROJECT 312131/2016-0 and process number 42098/2017-5) for the partial financial support.

References

[1] Apparatus for production of three-dimensional objects by stereolithography , C.W. Hull, US Patent 4575330A, August 1984

[2] Apparatus and method for creating three-dimensional objects (A system and a method for building three-dimensional objects in a layer-by-layer manner via Fused Deposition Modeling), S. Scott Crump, US Patent 5121329, June1992.

[3] **2015 Proceedings of PICMET '15: Management of the Technology Age 3D Printing: On Its Historical Evolution and the Implications for Busin** Elizabeth Matias, Bharat Rao New York University Polytechnic School of Engineering, Technology Management and Innovation Department, New York, NY – USA 551-558

[4] Turner Innovations. **High density compounds for 3d printing**. US nº US20160289468A1, 22 nov. 2013, 6 out. 2016. .

[5] Matheus Savi; Marco Antônio Bertoncini de Andrade; Jurgen Sand. **FILAMENTO RADIOPACO PARA USO EM IMPRESSÕES 3D**. BR Patent nº BR1020190131179, 24 jun. 2019

[6] IEC 61267: MEDICAL DIAGNOSTIC X-RAY EQUIPMENT - RADIATION CONDITIONS FOR USE IN THE DETERMINATION OF CHARACTERISTICS, 2005

[7] PUNNOOSE, J. et al. spektr 3.0 – A computational tool for x-ray spectrum modeling and analysis. **Medical physics**, v. 43, n. 8Part1, p. 4711-4717, 2016.